

## 4-8-2 Time Comparison Equipment for ETS-VIII

— Data Processing, Analysis and Capability of Time Comparison —

NAKAGAWA Fumimaru, IMAE Michito, TAKAHASHI Yasuhiro,  
KIUCHI Hitoshi, GOTOH Tadahiro, and FUJIEDA Miho

Engineering Test Satellite VIII (ETS-VIII) is planning to be launched in 2004 for fundamental studies on satellite positioning technologies and is the one first to be installed a highly precise cesium clock. To measure the clock offset between the satellite and the TCE Earth station, Time Comparison Equipment (TCE) has been developed in the CRL. The TCE will be used to improve TWTFT (Two Way Time and Frequency Transfer) and to measure both code and carrier phases. It is possible to compare two clocks with high precision. Moreover, TCE and TCE Earth stations have abilities to remove the delay by terrestrial ionosphere or in the receivers and transmitters.

From the examinations using TCE-EM (Engineering Model), we confirmed that TCE is able to measure the phases of clock with precision of a few nanoseconds by code observation and of a few picoseconds by carrier phase observation. Using these results, we estimated errors of time correction and found that TCE can perform on the TWTFT with high precision.

### *Keywords*

ETS-VIII, Satellite positioning, Time transfer, Atomic clock

### 1 Introduction

The Engineering Test Satellite VIII (ETS-VIII), scheduled for launch in 2004, has been developed to expand the advanced fundamental technologies required in future space exploitation, including mobile communications technology and high-precision satellite positioning technology [1]. This will be the first Japanese satellite to be equipped with an onboard atomic clock (the High Accuracy Clock: HAC) for use in the establishment of the basic technologies of a satellite positioning system. The Communications Research Laboratories (CRL) has developed Time Comparison Equipment (TCE) for time transfer between the atomic clocks on the satellite and on the ground, and plans to evaluate the characteristics of the atomic clock in orbit.

The TCE and the TCE earth station will conduct two-way time transfer between the atomic clocks on the satellite and on the ground. TCE and TCE earth station are designed to process data simultaneously to enable correction of the problematic delays in time transfer; namely, the fluctuation in equipment delay and in delay due to the terrestrial ionosphere. This correction is expected to provide higher overall precision in time transfer. The data collected by the TCE and TCE earth station are transferred to the data-processing units installed in the earth station, where correction and time-transfer processing is then performed.

This paper presents the configuration of the TCE and the principles of time transfer in Section 2, the details of the process in the data-processing unit in Section 3, and the

expected precision of time transfer based on test results using the TCE-EM (TCE-Engineering Model) in Section 4.

## 2 Two-way time transfer

### 2.1 Configuration

Figs.1 and 2 show the configurations of the TCE and of a TCE earth station, respectively. The TCE and TCE earth station perform time transfer using a ranging signal with spread modulation based on a Pseudo Random Noise (PRN) code, which functions in the same manner as the C/A code of GPS, and conducts measurement in two steps, one for the carrier phase and one for the code phase [2]. Both transmission and reception take place within the S-band, although the L-band is also used for one-way transmission from the satellite to the earth station. The transmission signal from the satellite to the earth is generated with reference to the onboard atomic clock.

The TCE operates with reference to the 10.23 MHz frequency and 1 kpps signals provided by the HAC, and measures the code and

carrier phases for the S-band reception signal, the S-band reception calibration signal, and the S-band transmission calibration signals. The reception calibration signal is generated in the TCE, superposed on the reception signal in the directional coupler at the antenna front end, and used to measure fluctuation in the delay within the receiver. The transmission calibration signal is generated by looping back the S-band transmission signal in the directional coupler at the antenna front end, and is used to measure fluctuation in delay within the transmitter. The measured values for these calibration signals are used to correct equipment delay.

The TCE earth station operates with reference to UTC (CRL). The earth station receives and measures the S-band and L-band ranging signal from the satellite and also generates and transmits the S-band ranging signal. TCE earth station measures the L-band reception calibration signals as well as the S-band reception calibration and S-band transmission calibration signals, which the TCE also measures. These calibration signals are used to correct equipment and ionospheric delays.

With the three sets of signal data measured by TCE (S-band reception, S-band reception calibration, and S-band transmission calibration signals) and the five sets of signal data measured by TCE earth station (S-band reception, S-band reception calibration, S-band transmission calibration, L-band reception, and L-band reception calibration signals), the data-processing unit conducts two-way time transfer and correction. Correction in the data-processing unit is designed to result in time-transfer precision on the order of several nanoseconds for the code phase, and precision of several picoseconds for the carrier phase; specifically, this is performed through resolution of the wave-number uncertainty problem via estimation based on code-phase information.

### 2.2 Principles of time transfer

First we will consider the code-phase time transfer. The code phase measured by TCE is

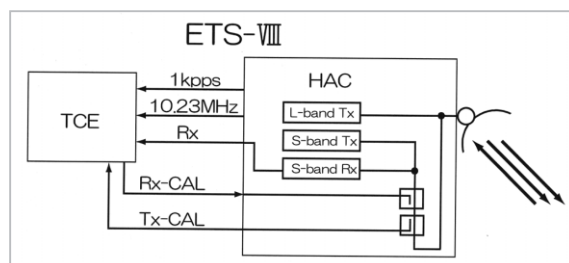


**Fig.1** Configuration diagram of TCE aboard the ETS-VIII

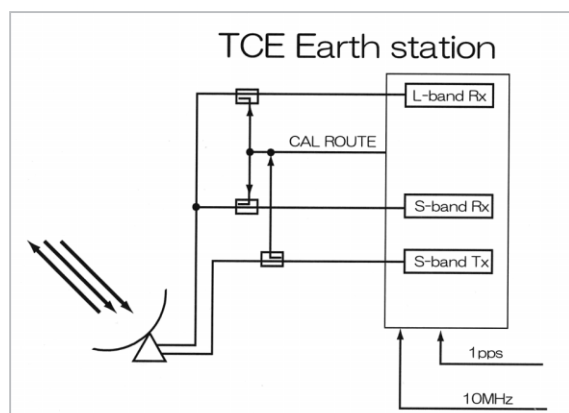


**Fig.2** Configuration of a TCE earth station

denoted as  $C^s$  and that measured by the TCE earth station is denoted as  $C_e$ . These are expressed as follows [3]:

$$C^s = \tau_g + dt^s - dt_e + I_u + T + d_{eTx} + d_{Rx}^s \quad (1)$$

$$C_e = \tau_g + dt_e - dt^s + I_d + T + d_{Tx}^s + d_{eRx} \quad (2)$$

Here, the symbols denote the following values:

$\tau_g$ : Transmission time (dependent on the distance between the satellite and the earth station)

$dt^s, dt_e$ : Time offset of the onboard atomic clock and UTC (CRL), respectively

$I_u, I_d$ : Uplink and downlink ionospheric delay, respectively

$T$ : Tropospheric delay

$d_{Rx}^s, d_{Tx}^s$ : Delay in the onboard receiver and transmitter, respectively

$d_{eRx}, d_{eTx}$ : Delay in the receiver and transmitter of the earth station, respectively

As the TCE measures the respective phases, wave-number uncertainty is generated. However, the code period can be as long as 1 ms, enabling estimation of the wave number based on orbital information (omitted in the above expressions). When the difference between these expressions is calculated,

$$C^s - C_e = 2(dt^s - dt_e) + (I_u - I_d) + (d_{Rx}^s - d_{Tx}^s) - (d_{eRx} - d_{eTx}) \quad (3)$$

is obtained, in which the transmission time (dependent on the distance between the satellite and the earth station) ( $\tau_g$ ) and tropospheric delay are cancelled out. Equation (3) still includes terms other than the time difference between the onboard atomic clock and UTC (CRL): specifically, it includes the difference between uplink and downlink ionospheric delay due to frequency differences and delay differences between the satellite receiver and transmitter and between the receiver and transmitter at the earth station. These delay values need to be eliminated, as we discussed in Section 3.

The carrier phases ( $\Phi^s, \Phi_e$ ) are expressed as follows, similarly to the code phase.

$$\Phi^s = \tau_g + dt^s - dt_e - I_u + T + d_{eTx} + d_{Rx}^s + \Phi^s(0) \quad (4)$$

$$\Phi_e = \tau_g + dt_e - dt^s - I_d + T + d_{Tx}^s + d_{eRx} + \Phi_e(0) \quad (5)$$

The ionospheric delay of the carrier phase is not a group delay; rather, it is a phase delay, which has the opposite sign as a group delay. As the carrier period can be as small as 400 ps, the initial phase terms ( $\Phi^s(0), \Phi_e(0)$ ) attributable to wave-number uncertainty, remain in the equations. As with the treatment of the code phase, the difference between expressions (4) and (5) is calculated as follows:

$$\Phi^s - \Phi_e = 2(dt^s - dt_e) - (I_u - I_d) - (d_{Rx}^s - d_{Tx}^s) - (d_{eRx} - d_{eTx}) + (\Phi^s(0) - \Phi_e(0)) \quad (6)$$

If the ionospheric delay differences and the receiver/transmitter delay differences in the code and carrier phase expressions could be removed, the initial phases of the carrier ( $\Phi^s(0) - \Phi_e(0)$ ) can be estimated from the code phase, since the time difference to be measured ( $dt^s - dt_e$ ) is the same for both code and carrier phases. If cycle slips do not occur within a set of experiments, the wave number during the experiment can also be obtained, since the initial phases are constant.

### 3 Data-processing

Two-way time transfer eliminates the effects of geometrical delay and tropospheric delay by calculating the difference between the values obtained at the TCE and at the TCE earth station for the code and carrier phases. However, this subtraction cannot remove ionospheric delay and the receivers/transmitter delay attributable to the difference in reception and transmission frequencies. The TCE and the TCE earth station are equipped to remove and correct these delays based on the data measured at the TCE and the TCE earth station, which is processed in the data-processing unit for correction and time transfer. In this section, this data-processing procedure is described, in process order (Fig.3).

#### (1) Doppler correction

The TCE divides the ranging signal into I and Q components, integrates the components

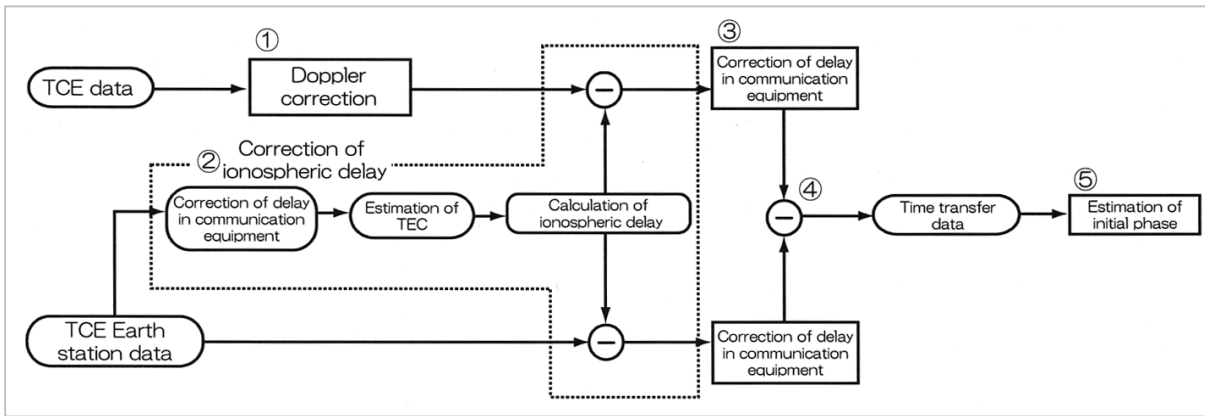


**Fig.3** Data-processing flow

for 1 second, and obtains the carrier phase from the arctan [2]. Thus, when Doppler frequency shift exceeds 1Hz, the integral approaches 0, and it becomes difficult to obtain the carrier phase. Thus, TCE earth station transmits the ranging signals with frequency correction, in order to cancel out this Doppler shift [4]. As a result, TCE measures the phase after correction, entailing the need for a process to recover the original frequency from the corrected frequency. Denoting the frequency corrected by the earth station at the time,  $t$  as  $\delta f(t)$ , the phase shift due to the Doppler correction,  $\phi(t)$ , can be calculated using the following expression:

$$\phi(t) = \int_0^t \delta f(\tau) d\tau \quad (7)$$

The TCE earth station will precisely measure the phase difference,  $\phi(t)$ , before and after Doppler frequency correction using DMTD (Dual Mixer Time Difference) [5] and will apply the obtained data to this correction.

(2) Correction of ionospheric delay

Group or phase delay,  $I(s)$ , attributable to the ionosphere is expressed as follows using the carrier frequency,  $f(\text{Hz})$ :

$$I = \pm \frac{1.345 \times 10^{-7}}{f^2} \int_L N ds \quad (8)$$

The positive sign corresponds to group delay and the negative sign corresponds to phase delay. Here,  $N(\text{m}^{-3})$  is the electron density. The integral on the right-hand side of the equation represents the integral of the elec-

tron density along the path and is referred to as the TEC (Total Electron Content). As the TCE uses different frequencies for uplink and downlink, the respective ionospheric delay values are different, and this has an effect on two-way time transfer (Table 1). As the code and carrier-phases have opposite signs (reflecting the difference between group delay and phase delay), determining initial phase is also problematic.

**Table 1** Ionospheric delay in uplink and downlink frequencies (in the direction of the zenith)

TEC	ionospheric delay	
	in the period of maximum solar activity, day time $1 \times 10^{18}(\text{m}^{-2})$	in the period of minimum solar activity, night time $3 \times 10^{16}(\text{m}^{-2})$
uplink (2656.390MHz)	19.0(ns)	0.57(ns)
downlink (2491.005MHz)	21.6(ns)	0.65(ns)
difference	2.6(ns)	0.08(ns)

As the TCE earth station uses two frequencies, one in the S-band and one in the L-band, to measure the time at which the ranging signals arrive, the station can estimate the TEC based on the difference in arrival times. At this stage, the initial phase of the carrier is still unknown; thus the code phase is used to estimate the TEC. The arrival time difference,  $C_{S-L}$ , between the S-band and L-band signals measured at a TCE earth station is expressed as follows:

$$C_{S-L} = (I_{Sd} - I_{Ld}) + (d_{STx}^S - d_{LTx}^S) + (d_{SeRx} - d_{LeRx}) \quad (9)$$

The second term on the right-hand side of the equation is the delay difference between the S-band and L-band transmitters of the HAC. The third term is the delay difference

between the S-band and L-band receivers of the TCE earth station. With the measured reception calibration data for the S-band and L-band signals, the TCE earth station can calculate the delay differences within the receiver using a method similar to that applied to delay correction in the communications equipment described in the next section. On the other hand, the satellite does not feature an L-band transmission calibration system and cannot conduct precise correction. However, the TCE conducts this correction using the delay difference in the HAC (measured in advance, under the assumption that this difference is constant). This correction can provide the difference between the S-band and L-band ionospheric delay  $\dot{C}_{S-L} = (I_{Sd} - I_{Ld})$ , and  $TEC(m^{-2})$  is calculated with the carrier frequencies  $f_S(\text{Hz})$  and  $f_L(\text{Hz})$ :

$$TEC = \frac{\dot{C}_{S-L}}{1.345 \times 10^{-7}} \times \frac{f_S^2 f_L^2}{f_S^2 - f_L^2} \quad (10)$$

Based on the TEC obtained here, delay is calculated for both frequencies and correction is performed to remove ionospheric delay.

### (3) Correction of delay in communication equipment

Next, delay is corrected in the receivers and transmitters of the TCE and the TCE earth station. The TCE and the TCE earth station measure both the transmission and reception calibration signals in the S-band, and the differences between these signals provide  $d_{Rx}^s - d_{Tx}^s$  and  $d_{eRx} - d_{eTx}$  in Equations (3) and (6), allowing for elimination of the effects of delay in the receivers and the transmitters.

Fig.4 shows an overview of the calibration system. The transmission signal is divided in the directional coupler at the antenna front end and returns to the TCE as the transmission calibration signal through the calibration path. On the other hand, the reception calibration signal is generated in the TCE, follows the calibration path, is superposed on the reception signal in another directional coupler, and returns to the TCE. The TCE earth station has similar calibration systems. The calibration path of an earth station passes through a cable,

and the transmission and reception calibration systems follow the same path. The TCE has different cables for transmission and reception calibration signals, but the cables run through the same locations and path lengths are assumed the same. Here, denoting the delay in the transmitter as  $d_{Tx}$ , the delay in the receiver as  $d_{Rx}$ , and the transmission time in the calibration path as  $\alpha$ , the times ( $T_{CTx}$ ,  $T_{CRx}$ ) measured in the transmission and reception calibration systems are expressed as follows:

$$T_{CTx} = d_{Tx} + \alpha \quad (11)$$

$$T_{CRx} = d_{Rx} + \alpha \quad (12)$$

Calculating the difference cancels out the transmission time in the calibration pathway,

$$T_{CRx} - T_{CTx} = d_{Rx} - d_{Tx} \quad (13)$$

The difference between receiver and transmitter delay can then be calculated, enabling the elimination of the effects of these delays.

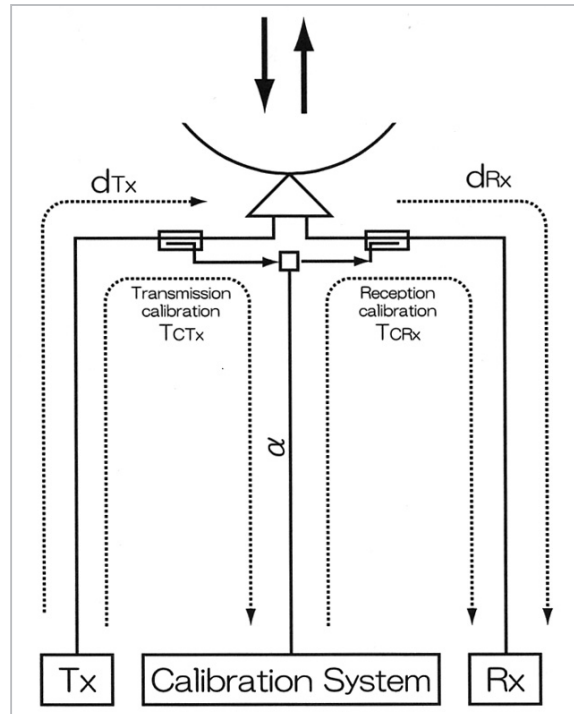


**Fig.4** Overview of the calibration system

### (4) Time transfer (5) Estimated carrier initial phase

The difference between the corrected data obtained by the TCE and the TCE earth station determines the difference between the onboard

atomic clock and UTC (CRL). Although the carrier-phase delay-difference data still includes the initial phase term, the initial phase of the carrier is estimated from the difference between the corrected code/carrier phases of the TCE and the TCE earth station, since the time difference in the measurement data is the same for both phases. This operation enables time transfer with the carrier phase.

#### 4 Time-transfer precision

This section discusses the precision of the time transfer and correction expected in actual experimentation, based on the measurement precision of the code and carrier phases.

##### 4.1 Measurement precision of TCE

To examine the measurement precision of the code and carrier phases for the TCE, the TCE-EM (EM: Engineering Model) was used for the testing configured, as shown in Fig.5. The test employed a hydrogen-maser atomic clock as the reference signal for the ranging

signal and either the same hydrogen-maser atomic clock or a Cesium atomic clock as the reference signal for the TCE. This test involved almost no variation of equipment delay and path-length. Thus, the measurement precision of the TCE-EM was measured when the reference signals for the ranging signal and for the TCE uses the same hydrogen-maser atomic clock, and the relative time difference between the hydrogen-maser and Cesium atomic clocks when the two reference signals use the above different clocks, respectively.

Fig.6 shows the code and carrier phases measured with the Cesium atomic clock for

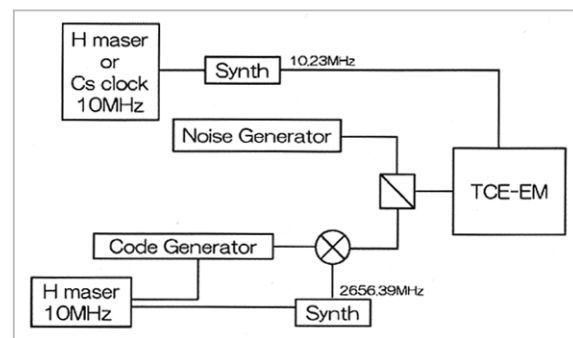


**Fig.5** Block diagram of the TCE-EM test

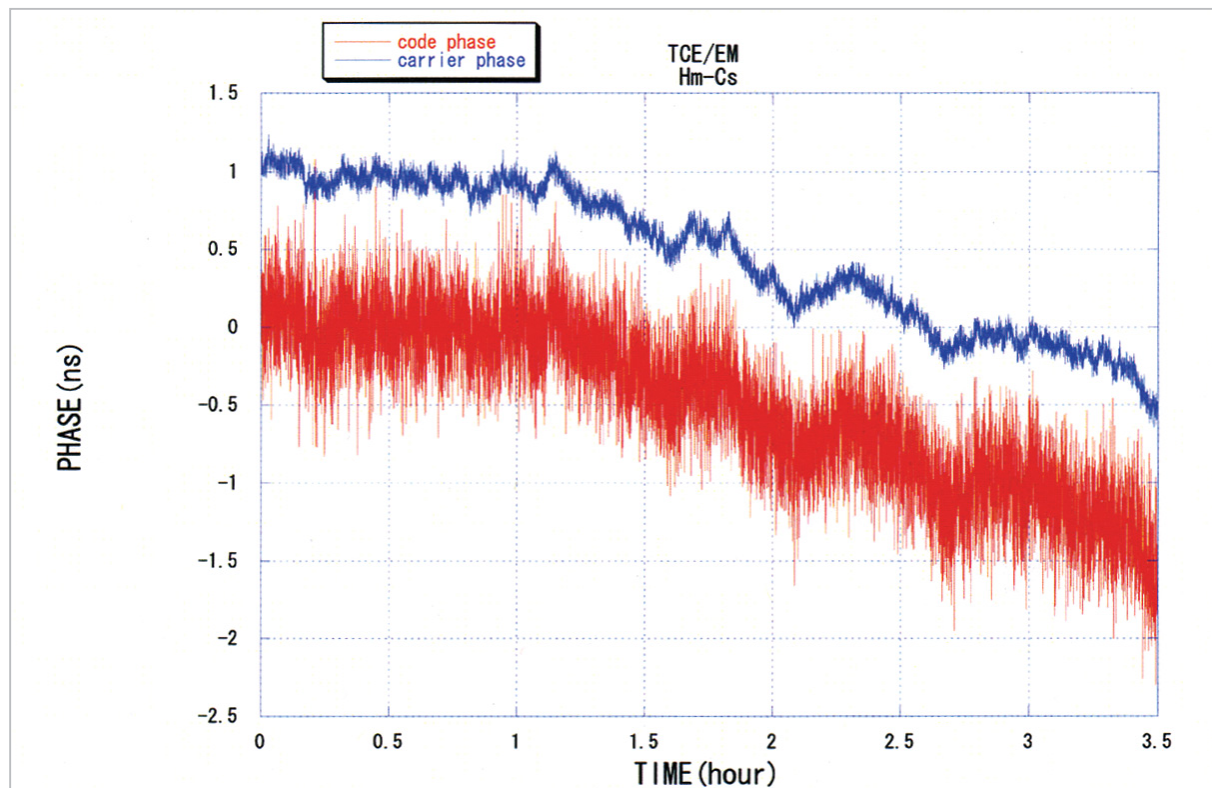


**Fig.6** Time-transfer test results for the hydrogen-maser and Cesium atomic clocks using the TCE-EM. Measurement with the code is indicated in red and carrier measurement is indicated in blue.

the TCE reference signal. The initial values for the code and carrier phases at  $t = 0$  are 0 and 1 ns, respectively. The code and carrier phases show the same tendencies in variation. It is clear that the carrier phase features precision on the order of several tens of picoseconds, which is close to the variance of the Cesium atomic clock, and that even the code phase demonstrates nanosecond-level precision.

Fig.7 shows the stability of the code and carrier phases during the test illustrated in Fig.6, system stability in carrier phase measurement, and the stability of the HAC. System stability for the measurement of the carrier phase for 1 second is  $1.0 \times 10^{-12}$ , which is extremely high, ensuring measurement on the order of picoseconds. Measurement with the code phase also reaches the stability of the HAC in approximately 1000 seconds, corresponding to sufficient precision in observation.

## 4.2 Precision of ionospheric delay correction

Let us consider the estimation precision of the TEC using two frequencies. Assuming that delay for the receiver and transmitter of the TCE earth station is completely removed, and considering only measurement error ( $\delta C_{S-L}$ ) in the arrival-time difference between the S-band and L-band signals, the error in TEC,  $\delta \text{TEC}$ , is expressed as follows:

$$\delta \text{TEC} = \frac{\delta C_{S-L}}{1.345 \times 10^{-7}} \times \frac{f_S^2 f_L^2}{f_S^2 - f_L^2} \quad (14)$$

Here, ionospheric delay correction error in the S-band,  $\delta I_S$ , is expressed as

$$\delta I_S = \frac{f_L^2}{f_S^2 - f_L^2} \delta C_{S-L} \quad (15)$$

Assuming the measurement precision of the code phase,  $\delta C_{S-L}$ , to be 1 ns (based on the test described in the previous section),  $\delta I_S$  is expected to be approximately 700 ps.

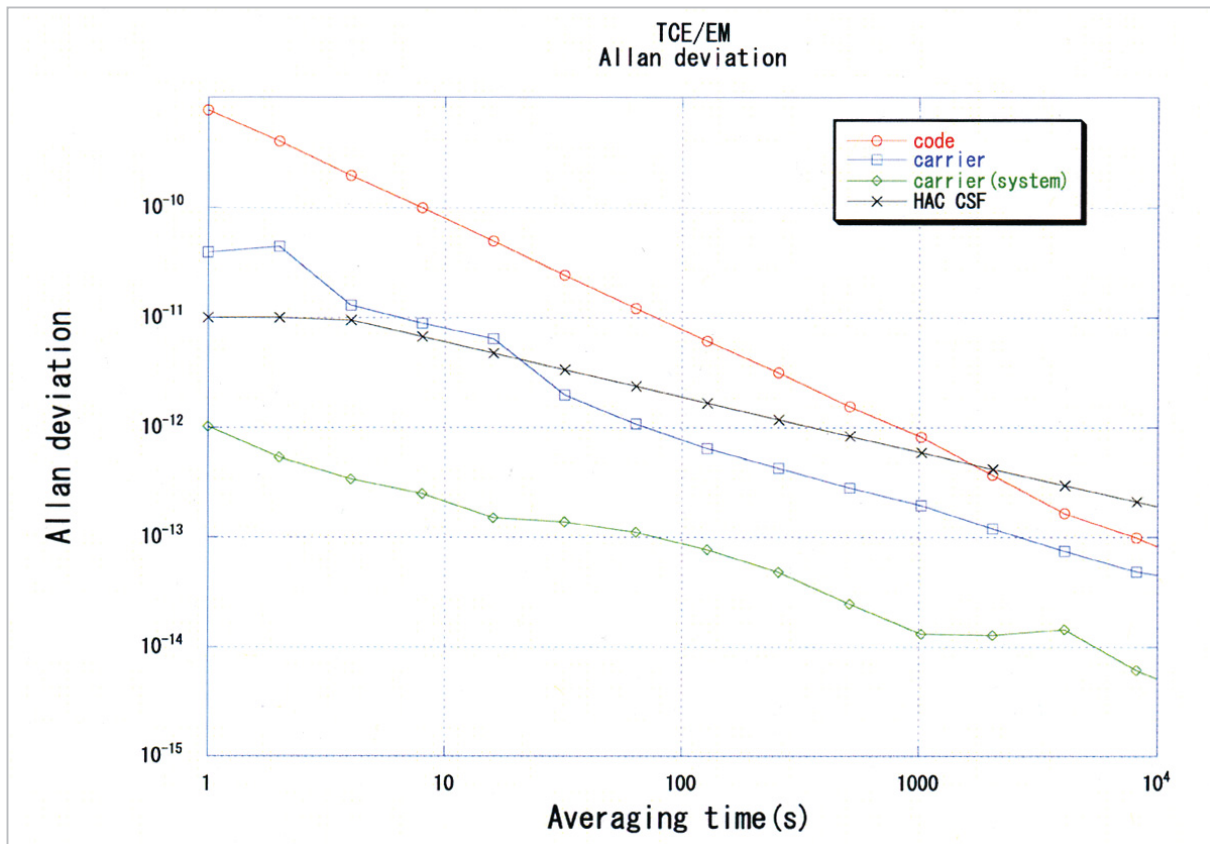


**Fig.7** Alan deviation for time transfer with the hydrogen-maser and Cesium atomic clocks.

The code phase is indicated in red and the carrier phase is indicated in blue. For reference, system stability in carrier-phase measurement is indicated in green and the stability of HAC is indicated in black.

This value corresponds to a measurement time of 1 second. Increasing the amount of data can reduce  $\delta I_S$ . Improvements are also expected in code-phase measurement precision for the earth station, improvements that are expected to increase the precision of the overall system even further.

### 4.3 Precision of initial-phase estimation

Based on the test results described in section 4.1, the precision of the initial-phase estimation for the carrier phase is calculated. Fig.8 shows the distribution function of the difference between the carrier and code phases. It is clear that the distribution is well-described by a normal distribution. The initial phase needs to be estimated only once in our experiment. Estimation precision depends on the given time for a single experiment. For example, if the experiment lasts 3 hours, 10800 data points are obtained. Here, the

interval estimation of the initial phase (confidence coefficient of 95%) yields precision of  $\pm 4.26$  ps, sufficient for the estimation of the initial phase.

## 5 Summary

The TCE and the TCE earth station measure the phases in the calibration system as well as the phases of the reception signals in two-way time and frequency transfer. The obtained data is transferred to the data-processing unit. We have shown that composite processing of the data in the data-processing unit can ultimately provide extremely high precision in time transfer. We also conducted a test with the TCE-EM, determined TCE measurement precision, and demonstrated based on the measured data that correction and estimation conducted in the data-processing unit provide sufficient precision.

The purpose of time transfer using the

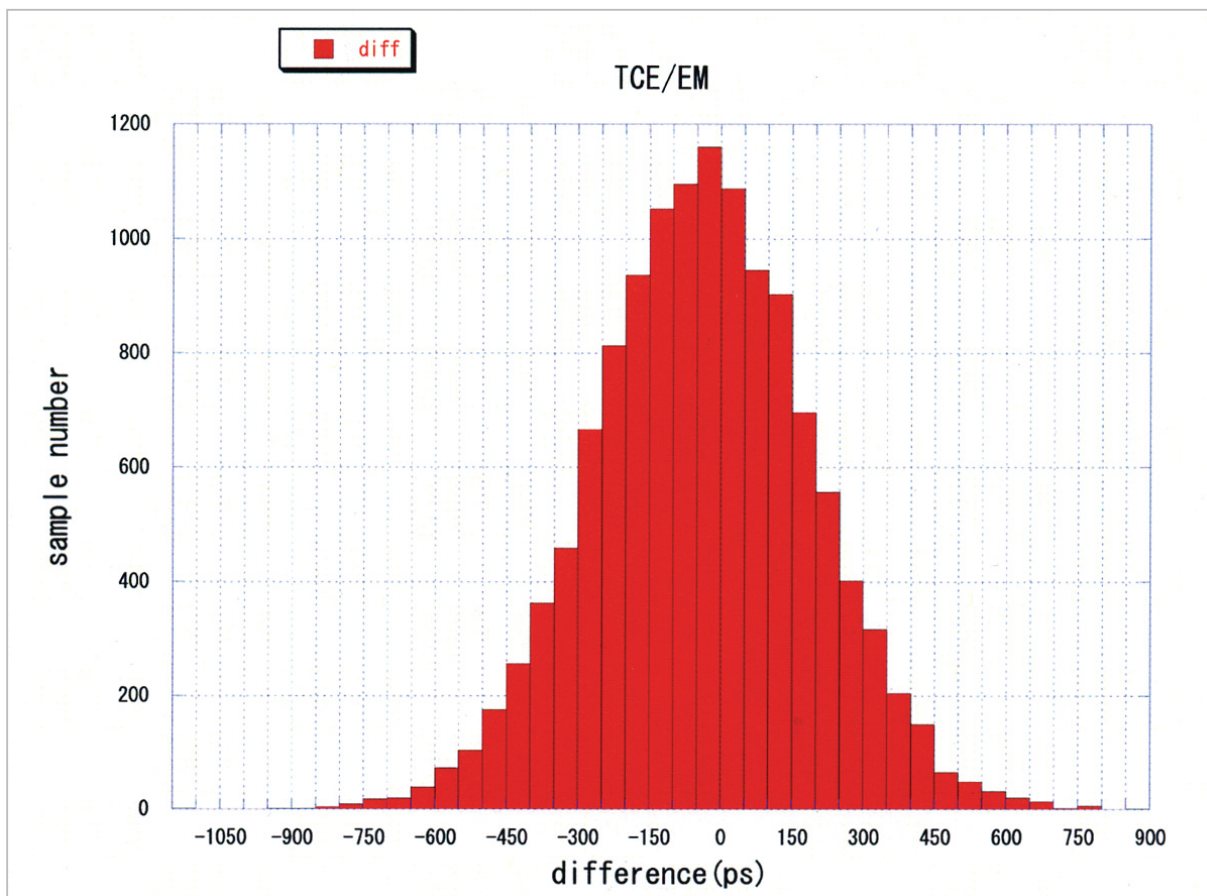


**Fig.8** Histogram illustrating the difference between the code and carrier phases.

The initial phase of the carrier is calculated based on these results.



TCE and the TCE earth station is to establish the basic technologies for satellite positioning systems, with high expectations for application to a quasi-zenith satellite planned for future launch.

## Acknowledgment

We would like to express our gratitude to Japan Communication Equipment Co., Ltd. for their help in the development and ground testing of the TCE.

## References

- 1 M. Homma, S. Yoshimoto, N. Natori, and Y. Tsutumi, "Engineering Test Satellite-8 for Mobile Communication and Navigation Experiment", IAF, No. IAF-00-M3.01, pp.256-263.
- 2 H. Kiuchi, M. Imae, Y. Takahashi, T. Gotoh, F. Nakagawa, M. Fujieda, and M. Hosokawa, "3-10-2 On-board Data Processing Part Time-Comparison-Equipment Processing Unit (TCE-PRO)", This Special Issue of NICT Journal.
- 3 P. J. Teunissen and A. Kleusberg, GPS for Geodesy, 2nd Edition, Sec. 5, Springer, 1998.
- 4 M. Fujieda, Y. Takahashi, T. Gotoh, F. Nakagawa, and M. Imae, "4-8-1 Earth Station of Time Comparison Experiment", This Special Issue of NICT Journal.
- 5 B. Komiyama, "SYUHASU TO JIKAN NO KEISOKUHO", Review of the Radio Research Laboratory, Vol.29, No.149, pp.39-53, 1983. (in Japanese)

### **NAKAGAWA Fumimaru, Ph. D.**

*Research Fellow, Time and Frequency Measurements Group, Applied Research and Standards Division  
Satellite Navigation, Satellite Time Transfer*

### **TAKAHASHI Yasuhiro**

*Senior Researcher, Time and Frequency Measurements Group, Applied Research and Standards Division  
Satellite Communication, Satellite Positioning System*



### **GOTOH Tadahiro**

*Researcher, Time and Frequency Measurements Group, Applied Research and Standards Division  
GPS Time Transfer*



### **IMAE Michito**

*Leader, Time and Frequency Measurements Group, Applied Research and Standards Division (present National Institute of Advanced Industrial Science and Technology)  
Frequency Standard, especially on Precise Time Transfer*



### **KIUCHI Hitoshi, Dr. Eng.**

*Senior Researcher, Optical Space Communications Group, Wireless Communications Division  
Radio Interferometry, Optical Space Communication*

### **FUJIEDA Miho, Ph. D.**

*Research Fellow, Time and Frequency Measurements Group, Applied Research and Standards Division  
Time Transfer, Satellite Navigation*

